

# Speed Control Strategies for E-AMAN using Holding Detection-Delay Prediction Model

Imen Dhief\*, Zhi Jun Lim\*, Sim Kuan Goh\*, Duc-Thanh Pham\*, Sameer Alam\* Michael Schultz†,

\*Air Traffic Management Research Institute, Nanyang Technological University, Singapore

†Institute of Logistics and Aviation, Dresden University of Technology, Germany

**Abstract**—Reducing flight delays is considered one of the biggest challenges of the air transportation system due to its far-reaching economic, operational, and environmental impact. Airlines and Air Navigation Service Providers (ANSPs) must collaborate to optimize their procedures in order to manage delays. The SESAR Solution, Extended Arrivals Manager (E-AMAN), allows for early sequencing of the flights, thereby reducing the aircraft holding times and thus managing congestion in Terminal Maneuver Airspace (TMA). However, there is a lack of methodological approaches for transferring the flight delays and holdings from the approach phase to the cruise phase. To this end, we have approached this problem using both data-driven and optimization techniques. First, we propose a method to detect the holding pattern/time from historical trajectory data. Then a prediction model is introduced to predict holdings and delays 200 NM from the airport. Finally, we develop an optimization model that takes the predicted delays as an input and provides the airlines/ANSPs with adequate speed adjustment, which can absorb delays in the approach phase and transfer them to the cruise phase. Results demonstrate that better prediction of holding pattern/time can lead to predicting the flight delays, in the approach phase, with high accuracy. Furthermore, the proposed speed control model shows that, with a speed reduction of less than 10% at 500 NM from the airport, up to 70% of the initial delays could be absorbed in the cruise phase. As a result, the average delay per flight (at the approach phase) is decreased from 6 minutes to almost 2 minutes.

**Keywords**—holding detection, extended AMAN, holding prediction, delay prediction, speed control, data-driven, optimization.

## I. INTRODUCTION

As airports are approaching their capacity limits, new decision support alternatives should be introduced in order to overcome the TMA congestion. Extended Arrival Management (E-AMAN) is one such concept developed in the frame of the SESAR Program (Single European Sky ATM Research) as an upgrade of the currently applied AMAN system [1]. E-AMAN assists ATC in the sequencing of arrival traffic in the cruise phase of flight, much earlier than AMAN horizon. The main concept is to reduce aircraft holding time in congested TMAs by managing their speed during the cruise phase of flight, usually 180-200 NM away from the airport. Controllers in the upstream sectors, which may be in a different control center, obtain system advisories to support an earlier aircraft's pre-sequencing. Controllers implement those advisories by, for example, instructing pilots to adjust the aircraft speed along the descent or even before top-of-descent, thus reducing the need for holding and decreasing fuel consumption. E-AMAN

validation trials have been performed in many cities such as Rome, Amsterdam, and London. Findings demonstrate that aircraft's fuel consumption is reduced by an average of 8% per flight; furthermore, the airborne waiting time is reduced by up to 90% [2].

Despite the substantial benefits expected from implementing the E-AMAN, an accurate prediction of flight arrival time/delays, especially in the terminal airspace with complex holdings, remains a challenge for its wider deployment. Moreover, by extending the coverage radius up to 500 NM, the uncertainties in estimating the arrival times raises. In fact, inaccuracies in arrival time computation cause a perturbation in the flight landing sequence due to flights coming before or after their estimated time of arrival. This may lead to the re-generating of delays at the TMA.

In this work, we propose a method for detecting and predicting flight holdings and predicting delays in TMA, with speed control strategy to absorb such delays in the cruise phase. As a case study, the proposed method is applied to reduce airborne delays for arrival traffic into Singapore Changi Airport (WSSS) by developing the concept and procedures augmenting the E-AMAN initiatives. The proposed methodology includes two independent but complementary approaches. The first approach focuses on predicting flight delays at an early stage (before reaching the Initial Approach Fix (IAF)), while the second permits to instruct the pilots (through upstream controllers or Airline Operations Office) with the speed change advisory to absorb this delay. To this end, we make use of data-driven methods together with optimization techniques.

The main contribution of this paper are:

- A holding detection method to detect, from historical flight data, any flight holdings in TMA and their duration.
- A holding prediction model that determines, at 200 NM from the airport, whether a flight will enter a holding pattern or not (Classification problem). This probability function is fitted to a prediction model that predicts the flight time of holdings (Regression problem).
- A delay prediction model that takes the predicted holding time as an input and predicts, at 200 NM from the airport, the flight delays encountered in the approach phase.
- A speed control strategy to absorb the predicted delays in the cruise phase.

The paper is organized as follows. First, section II includes a literature review summarizing the previous main works that belong to the scoop of our topic and our proposed



approach. The data preparation and exploration are highlighted in section IV. Subsequently, section V and section VI describe in details the proposed prediction models and speed strategy model, respectively. Section VII discusses the computational results. Finally, conclusions are drawn in section VIII.

## II. BACKGROUND

Effective implementation of E-AMAN requires an accurate prediction of delay in the approach phase and effective delay absorption mechanism such as speed control strategy.

### A. Delay prediction

Predicting the delay in the approach phase is a challenging problem due to the non-deterministic nature of both environmental and air traffic factors, including wind uncertainties, inaccuracy of in-flight parameters, and frequent tactical vectoring of the flight trajectory by TMA controllers. Delay in the approach phase is defined as the difference between the actual and planned duration the aircraft flies from the initial approach fix to landing. It is similar to the arrival/ landing time prediction (LDT), which involves predicting the transit time in the TMA.

Recently, due to their effectiveness in dealing with uncertainty and prediction problem, machine learning approaches, for predicting LDT have been proposed. For example, Glina et al. [3] apply Quantile Regression Forests (QRF) to estimate aircraft landing times. Their findings consist of a short-term prediction (with a radius of prediction ranging between 20-30 NM) of flight arrival times with an accuracy of about 60 seconds for 68% of flights. In the same context, [4] presented a short-term trajectory prediction in TMA based on 4D trajectory prediction. Their model consists of data mining and Deep Neural Networks (DNNs) model. They predict the LDT at the TMA (within 25 NM from the airport) with an MAE of 70 seconds.

In data-driven LDT prediction research feature selection is a critical a process of transforming raw data into features that better represent the underlying problem to the predictive models, resulting in improved model accuracy on unseen data. In [5] improved the Estimated Time of Arrival (ETA) predictions by intensive feature analysis using Random Forest (RF), with an accuracy of 78.8% than the FAA's ETMS.

One research gap in the previous work for predicting transit time or delay in TMA is the lack of consideration of holding time as one of the features for delay prediction. Aircraft that undergo holding experience extra flight time and elongated flight distance; hence, this affects their transit time/ delay in the approach phase. Therefore, in our work, we include a holding prediction model to predict the holding time in the approach phase and utilize the predicted holding time to predict delay. In order to build a holding prediction model, we first have to develop a holding detection algorithm by studying the holding patterns of the flights using flight data. Another research gap in the previous work is the limited prediction horizon for predicting transit time or delay in the TMA. In our work, we

propose to predict the approach phase delay when the aircraft is at 200 NM away from the airport.

Furthermore, the prediction of flight delays, in itself, does not provide quantitative insight into improving the TMA operational performance. Thus, we implement a speed control strategy aiming to absorb the predicted delay at the cruise phase so that the approach outcome can be evaluated in terms of reducing delays and congestion in the TMA.

### B. Speed control for Air Traffic Flow Management

Several researchers have investigated the implementation of a speed control strategy for Air Traffic Flow Management (ATFM) purposes. In [6], Delgado et. al proposed a cruise speed reduction strategy to complement ATFM ground delay. Results show that given a nominal cruise speed, there exists a bounded range of speeds reduction (5% to 12%) that allows aircraft to fly slower with the same or lower fuel consumption than the nominal flight.

A recent work by Yoshinori et al. [7] proposes a detailed analysis of the achievable airborne delays by speed control. They show that around 2 to 3 minutes of delays per each 30 minutes of flight time could be achieved by a speed reduction while saving about 2 – 3% of fuel consumption. Further, Jones et al. [8] presented an approach to transfer delay from the TMA airspace to the cruise phase by adjusting the flight speeds during the cruise phase in order to avoid any trajectory adjustment such as vectoring, speed change, or holdings at the TMA airspace. The authors propose to consider flights at a radius of 500 NM from the airport and instruct them with a Controlled Time of Arrival (CTA) to a metering fix situated at approximately 150 NM from the airport. The results show a transfer of up to 20% of the delays from the terminal area to the cruise phase of the flight. Another important finding in this work is that part of delays can be transferred into the cruise phase, even with only 25% of compliant flights. However, the aircraft's actual flight profile is subject to several external operational uncertainties such as weather and airport congestion, which are not considered in their model.

## III. PROPOSED APPROACH

This research work proposes to combine two independent models, flight delay prediction and speed control strategy, to demonstrate benefits of E-AMAN.

- The first model focuses on predicting the flight delay in the approach phase. In the feature engineering process, we include features reported in our recent work [9]. As flight holdings influences the flight transit time, and thus contributes to flight arrival delays we have included the holding pattern in our prediction model. Furthermore, we propose the prediction model at 200 NM from the airport.
- The second model consists of a speed control strategy to absorb the predicted delays at the cruise phase. Since our goal is to absorb delays, we restrict our speed control maneuver to slowing down the aircraft speed. As most of the discussed literature in the speed control strategy suggests, two speed reduction ranges are considered:



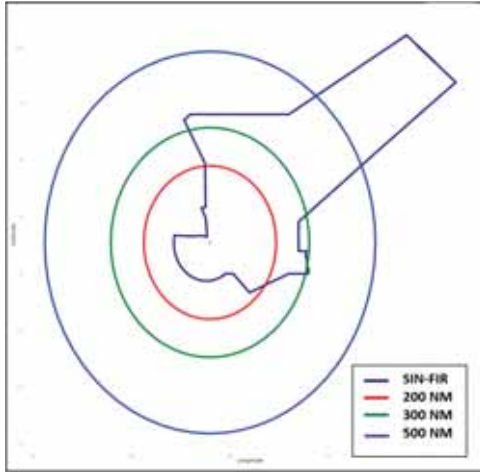


Figure 1. Range rings and Singapore FIR

less than 10% and between 3% to 6%. Furthermore, we consider studying three different radius coverage from the airport, namely 200 NM, 300 NM, and 500 NM. Therefore, virtual concentric circles centered around Singapore Changi airport are considered, referred to as Range Rings (RR), as illustrated in Figure 1.

Our proposed methodology is highlighted in Figure 2. It includes four main models that are performed sequentially, each of which inputs the preceding model outputs. The first block is a data mining model that involves cleaning the data, detecting the trajectory with holdings, and extracting the features relevant to the prediction model. The second model is the holding time prediction model. It combines two prediction models: the first is a classification model to predict whether the considered flight will be on holding or not, while the second is a regression model to predict the holding time. The third block is the delay prediction model. The last model includes the speed control strategy.

#### IV. DATA

##### A. Data source

The data used in this work is related to arrival flights to Singapore Changi Airport (ICAO: WSSS) for the month of May of 2019. They are collected from the following sources:

1) *Air Traffic data*: The 4D trajectory data source of this study is Automatic Dependent Surveillance-Broadcast (ADS-B) flight data derived from the OpenSky Network [10]. Flight plans are derived from a major airline in Southeast Asia with flight arrivals into Singapore Changi Airport.

2) *Meteorological data*: The meteorological data (METAR) for Singapore Changi airport station are extracted from of Iowa Environmental Mesonet from Iowa State University [11].

##### B. Data Processing

Data Processing involves two steps noise filtering and outlier removal. In the noise filtering step, we remove duplicated flights, flights with incomplete trajectory or flight plan data and flights which originates within 200 NM range ring of destination airport (WSSS) as there will be insufficient time in the cruise phase to apply speed control.

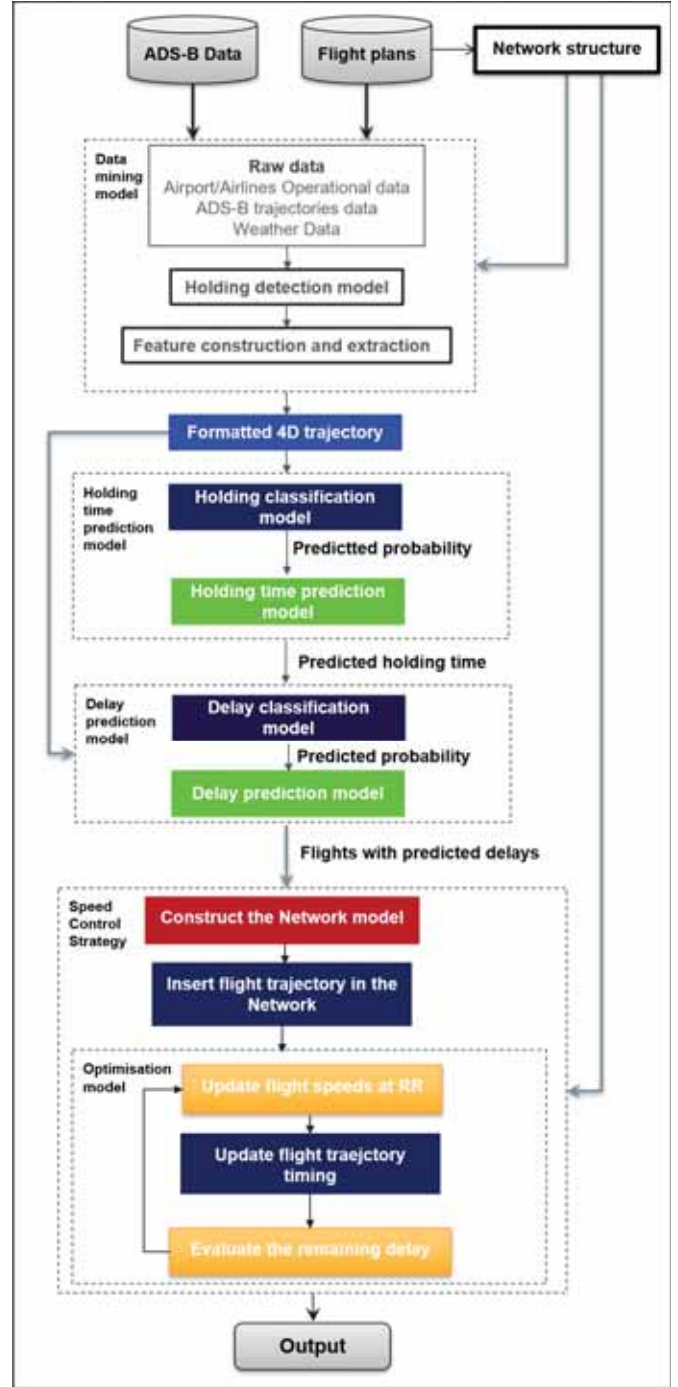


Figure 2. Methodology framework

In addition, data which has holding time or approach phase delay which are two standard deviations away from the respective average values are considered as outliers and thus are removed from the dataset. After outliers removal, we are left with 9376 flights with 2091 having flight plans.

#### V. HOLDING & DELAY PREDICTION FRAMEWORK

The delay prediction framework (as illustrated in Figure 2) predicts the delay of each aircraft in the approach phase when the aircraft is at the range ring (i.e., 200 NM away from the airport) so that the flights can adjust their speed in the

remaining cruise phase to absorb the predicted delay in the approach phase. The prediction point is labeled in Figure 6, and the speed control strategy are outlined in Section VI. The framework consists of features extraction and construction, holding detection and prediction, and delay prediction.

### A. Feature Extraction & Construction

Table I presents the list of possible features that are included in the holding and delay prediction models.

Instead of considering the individual components of the weather parameters and phenomenon as separate features of the prediction models we used Air traffic management airport performance (ATMAP) weather algorithm [12] by Eurocontrol to generate a representative index which indicates the severity of the overall weather conditions in Air Traffic Management.

As there are four runways available for commercial flights landing and departing in Singapore Changi Airport are 02L, 02C, 20R, and 20C. The arrival demand is computed using the estimated time of arrival of the landing flights, and the departure demand is computed using the estimated time of departure of the departing flights.

### B. Holding Detection Model

A holding pattern can be characterized by an oval course, which is an intrinsic property that differs, holding from other types of maneuvers. In kinematics, the projection of 4D holding trajectories onto its flight path undergoes oscillation. Based on this property, we can perform the segmentation of a 4D trajectory into segments with and without holdings. This can be achieved by detecting zero crossings in speed from the projected motion, estimated by Kalman filter (KF). Holding time is computed based on the start and end time of a segmented holding trajectory.

The input of the holding detection algorithm are:

- A flight trajectory is defined by a set of discrete points, which are interpolated each 1 second. Let us consider the trajectory point as the set  $(X(t), Y(t))_{t \in [0, \dots, n]}$ , where  $n$  is the flight points number.
- An associated flight path defined by a set of segments.

Figure 3 shows an example of a flight trajectory fragment where holding is detected, with the flight path segment.

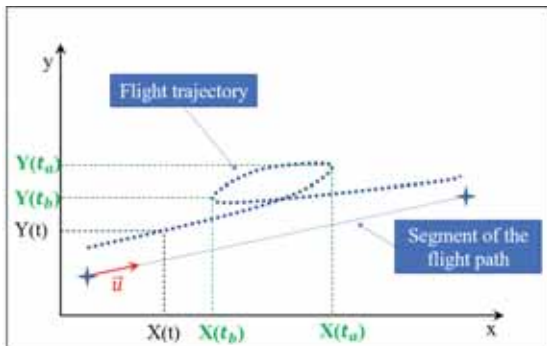


Figure 3. Example of a flight holding pattern for the holding detection.

The steps of the holding and holding time detection algorithm are enumerated as follows:

- 1) The KF estimates the flight velocity components at each trajectory point, as follows:

$$[X, Y, \dot{X}, \dot{Y}] \leftarrow \text{KF}(X, Y) \quad (1)$$

- 2) The projection  $V_u(t)$  of the aircraft velocity vector  $(\dot{X}(t), \dot{Y}(t))$  on the flight path (where  $\vec{u}$  is its unit vector as shown in Figure 3). This provides us longitudinal speed along the flight path. It is computed by:

$$V_u(t) = \begin{bmatrix} \dot{X}(t) \\ \dot{Y}(t) \end{bmatrix} \cdot \vec{u} \quad (2)$$

An example of the variation of the speed component  $V_u$  in case of a detected holding is highlighted in Figure 4.

- 3) If the vector  $(V_u(t))_{t \in [1, \dots, n]}$  includes a sequence of negative values for more than  $T_n$  seconds, a holding is detected. Otherwise, a flight trajectory is without holding.  $T_n$  is empirically chosen to be 30 seconds.
- 4) If a holding is detected, the time of holding is derived by computing the first turn around time  $t_a$  and the second turn around time  $t_b$  that verify equation 3 and 4, respectively. This can be computed from the zero-crossings in speed such as in Figure 4. Equation 3 computes the first time  $t_a$  where  $(V_u(t))_{t \in [1, \dots, n]}$  goes to negative values. Equation 4 computes the first time  $t_b$  where  $(V_u(t))_{t \in [t_a, n]}$  goes back to positive values after  $t_a$ .

$$t_a = \min_{t \in [1, \dots, n]} t \text{ s.t. } V_u(t) < 0 \quad (3)$$

$$t_b = \min_{t \in [t_a, \dots, n]} t \text{ s.t. } V_u(t) > 0 \quad (4)$$

- 5) Finally, the time between  $t_a$  and  $t_b$  represents half of the holding time. Thus, the holding time  $T_h$  is given by:

$$T_h = 2 \times (t_b - t_a) \quad (5)$$

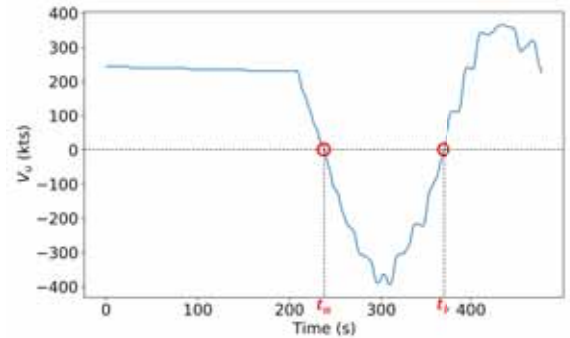


Figure 4. Variation of the speed component  $V_u$  relative to time

### C. Machine Learning Algorithm for Predictive Models

We have adopted CatBoost machine learning algorithm which deploy gradient boosting on decision trees, with categorical features support [13] for Holding Prediction and Delay Prediction models.

TABLE I. SUMMARY OF ALL POSSIBLE FEATURES

Type	Name	Description
Flight Information	Origin Region	First letter of ICAO airport code of departure airport
	Wake	Wake category of aircraft (e.g. H , M)
Flight parameters at range ring	Latitude	Latitude of aircraft when it enters the range ring
	Longitude	Longitude of aircraft when it enters the range ring
	Altitude	Altitude of aircraft when it enters the range ring
	Heading	Heading of aircraft when it enters the range ring
	Ground Speed	Ground Speed of aircraft when it enters the range ring
	HOD	Hour of the day when aircraft enters range ring
Flight paths	DOW	Day of the week when aircraft enters range ring
	Airway	Planned airway of the aircraft
	STARS	Planned Standard Terminal Arrival Route of the aircraft
Surrounding Traffic	Runway	Planned landing runway of the aircraft
	Before_30	Number of aircraft that entered .the range ring in the past 30 minutes
	After_30	Number of aircraft expected to enter the range ring in the next 30 minutes
Weather	Average Speed	Average speed of aircraft that enters the range ring 30 minutes before and after
	Weather Index	ATMAP weather index of weather 1 hour after aircraft enters range ring
Airport Performance Metric	Arrival_02L	Estimated number of landing flights on Runway 02L 1 hour before aircraft's ETA
	Arrival_20R	Estimated number of landing flights on Runway 20R 1 hour before aircraft's ETA
	Arrival_02C	Estimated number of landing flights on Runway 02C 1 hour before aircraft's ETA
	Arrival_20C	Estimated number of landing flights on Runway 20C 1 hour before aircraft's ETA
	Departure_02L	Estimated number of departing flights on Runway 02L 1 hour before aircraft's ETA
	Departure_20R	Estimated number of departing flights on Runway 20R 1 hour before aircraft's ETA
	Departure_02C	Estimated number of departing flights on Runway 02C 1 hour before aircraft's ETA
Departure_20C	Estimated number of departing flights on Runway 20C 1 hour before aircraft's ETA	

1) *Holding Prediction Model*: There are two parts to the holding prediction model, as shown in Figure 2. The first portion is the holding classification model, and the second portion is the holding time prediction model. The purpose of the holding classification model is to predict the probability of holding for each flight in the approach phase, and the prediction horizon is also at 200 NM away from the airport. The predicted probability of the holding is then utilized inside the holding time prediction model. The holding time prediction model is a regression model, and it predicts the total time that an aircraft will undergo airborne holding in the approach phase when the aircraft is at the 200 NM range ring. The output of the holding prediction model (i.e., predicted holding time) is an important input for the delay prediction model.

2) *Delay Prediction Model*: In order to build the delay prediction model, we first have to extract the delay information from each flight trajectory. The actual duration in the approach phase can be extracted from the ADS-B data, while the planned duration can be extracted from the flight plan. Therefore, delays are not only computed for flights with holdings but vectored flights are also considered. Furthermore, only flights with both ADS-B data and flight plans are used in building the delay prediction model. As a result, the delay prediction model is specific to just one airline which flight plan is available.

Similar to the holding prediction model, the delay prediction model also consists of two parts, which are the delay classification model and the approach delay prediction model, as shown in Figure 2. The delay classification model predicts whether a flight will experience a delay of greater than two minutes in the approach phase when the aircraft is at the RR 200 NM. This delay classification model employs the predicted holding time from the holding prediction model. The predicted probability of delay greater than two minutes for each flight is then extracted from the model, and this information is included in

the approach delay prediction model. The reason for choosing 2 minutes as the boundary for deciding whether the flight has delay is to take into account for the noise present in the ADS-B data. The approach delay prediction model is a regression model, and it predicts the total delay of an aircraft in the approach phase when the aircraft is at the RR 200 NM. Other than utilizing the predicted probability of delay greater than two minutes, the approach delay prediction model also includes the predicted holding time from the holding prediction model as one of the features.

## VI. SPEED STRATEGY TO ABSORB APPROACH PHASE DELAYS

The speed control strategy is a mechanism implemented in order to absorb the predicted delays that are derived from the model presented in Section V. The main objective here is to transfer delays from the approach phase to the cruise phase. First, we implement a network structure that permits to represent the considered airspace and model effectively the flight trajectories. Thus, the mechanism of inserting the ADS-B trajectories into the proposed network is also discussed in detail. Then, the problem formulation is displayed, including and explicit definition of the input data used, the speed strategy applied, the conflict detection model, and the optimization problem formulation proposed.

It is worth mentioning that our approach does not focus on eliminating the delays for two main reasons. First, canceling delays require a rescheduling of the airport resources allocation. Second, due to the increase in traffic density, flight arrival delays are becoming inevitable even with an optimal allocation of runways and taxiways. Alternatively, the current work aims to clear the flight approach phase from delays by shifting delays to the cruise phase. Our proposed approach does not achieve a benefit in terms of flight time; meanwhile, it contributes to reducing congestion in the terminal area.

Therefore, the flight landing times are maintained as initially instructed by ATC, and thus, no re-sequencing is required. Moreover, our approach requires further cooperation between different involved Area Control Centers(ACC). This is facilitated by the System Wide Information Management (SWIM) that consists of a shared platform to harmonize information exchange between all the involved airspace users.

#### A. Network model

The airspace is considered as a structured graph  $\mathcal{G}(\mathcal{W}, \mathcal{L})$ , where  $\mathcal{W}$  is a set of waypoints (Wps), and  $\mathcal{L}$  is the set of links (Ls) associating each two consecutive Wps. Each Wp is defined by its latitude, longitude, and altitude. The set of subsequent Wps reaching the Final Approach Fix (FAF) is called Flight Paths (FPs). For each range ring (Figure 1), a subset of the graph network is considered.

1) *Inserting ADS-B trajectories in the network:* To associate ADS-B trajectories to the network FPs, we apply the Dynamic Time Wrapping (DTW) distance metric. It permits to compute the distance between two trajectories having a different number of points. Figure 5 illustrates an example

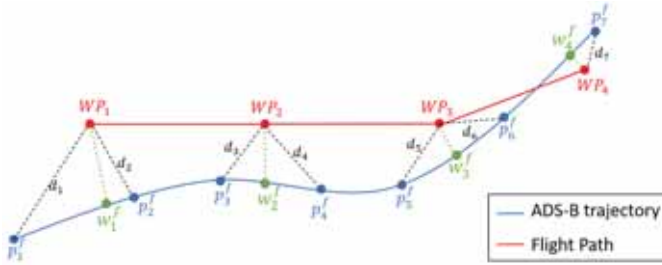


Figure 5. Mapping ADS-B trajectory with FP

of how we map ADS-B trajectory (solid blue line) with a FP (solid red line). Let us consider a flight  $f$  having an ADS-B trajectory defined by  $(P_j^f)_{j \in [1..m^f]}$ , where  $m^f$  is the number of the trajectory points, and a FP defined by  $(WP_j)_{j \in [1..n^f]}$ , where  $n^f$  is the number of waypoints.

The DTW distance between  $(p_j^f)_{j \in [1..m^f]}$  and  $(WP_j)_{j \in [1..n^f]}$  is defined as  $\sum_{i=1}^{m^f} d_i$ , where  $d_i$  (dashed black line in Figure 5) represents the distance between  $(p_i^f)$  and the closest point in  $(WP_j)_{j \in [1..n^f]}$ . Thus, for each flight  $f$ , the DTW with all the FPs is computed. Then, the closest FP to  $f$  trajectory is assigned to  $f$ .

Once each ADS-B trajectory is associated with a FP, the orthogonal projection of the FP waypoints into the ADS-B trajectory is determined and referred to as associated waypoint  $(w_j^f)_{j \in [1..n^f]}$  (See Figure 5). Thus, the time needed to fly between each two consecutive waypoints  $WP_k$  to  $WP_{k+1}$  is defined by the time recorded between  $w_k^f$  and  $w_{k+1}^f$ . By associating each ADS-B trajectory with its corresponding FP, in the sequel, each flight trajectory is limited to the set of points  $(w_j^f)_{j \in [1..n^f]}$  for each flight  $f$ .

#### B. Problem formulation

Let us consider a set of flights  $\mathcal{F}$  arriving to the considered airport. Each flight  $f \in \mathcal{F}$  includes the following input data:

- Associated flight path:  $(WP_j^f)_{j \in [1..n^f]}$ , where  $WP_j^f$  is a 3D point defined by its latitude, longitude and altitude.
- Actual trajectory points associated with the flight path:  $(w_j^f)_{j \in [1..n^f]}$ , where  $w_j^f$  is a 4D point defined by its latitude, longitude, altitude, and time.
- The flight speed profile  $(v_j^f)_{j \in [1..n^f]}$ , where  $(V_j^f)$  is the speed of  $f$  at the trajectory point  $w_j^f$ . The speed profile is extracted from the actual trajectory, and it is assumed to be the agreed speed between pilots and ATC. In the current work, we assume that ATC instructs this speed profile at each flight path waypoint, and it is considered as input data to our model.

The current work is tackling the problem of flight arrival delays from the airline perspective. Therefore, the speed control strategy is not applied to the entire flight set; rather, it is dedicated to a particular airline. The flight set is subdivided into two groups, as follows:

- Cooperative Flights ( $\mathcal{CF}$ ) are flights belonging to the major airline operating in south-east Asia. They are capable of communicating with the Singapore ANSP and get the required instructions. Furthermore, as we only consider flights with a delay more than 2 minutes in the speed control process, all flights belonging to  $\mathcal{CF}$  are predicted to be delayed by more than 2 minutes and are involved in the speed control strategy.
- Non-Cooperative Flights ( $\mathcal{NCF}$ ) are arriving flights that are not considered in the speed control maneuvers.

Our objective is to reduce arrival delays for only  $\mathcal{CF}$  flights. Therefore,  $\mathcal{CF}$  flights are required to adjust their speeds in the cruise phase in order to absorb approach phase delays while avoiding conflicts with both  $\mathcal{CF}$  and  $\mathcal{NCF}$  flights.

1) *Speed control strategy:* The proposed approach is illustrated in Figure 6. Let us consider a flight  $f$  entering the RR at  $t_0^f$  and reaching the Initial Approach Fix (IAF) at  $t_{n^f}^f$ . If  $f$  is predicted to be delayed by a time  $D^f$  at its approach phase, our objective is to revise  $f$  speed so that the assigned delay is progressively absorbed before reaching the IAF. Thus,  $f$  have to reach each waypoint  $w_i^f$  at  $(t_i^f + \delta_i^f)$ , where  $t_i^f$  is the original time over  $w_i^f$  and  $\delta_i^f$  is the achieved delay when slowing down the aircraft from  $w_{i-1}^f$  to  $w_i^f$ . Therefore, the aggregate value of the elementary delay  $\delta_i^f$  has to be equal to the initial delay  $D^f$ .

In order to compute the flight timing over the waypoints after changing the aircraft speed, we assume that the aircraft perform a constant deceleration. For instance, let us consider an aircraft  $f$  flying from  $w_j^f$  to  $w_{j+1}^f$  with a speed  $v_j^f$  and  $v_{j+1}^f$ , respectively (Figure 6). The constant speed deceleration  $a(t)$  is a function of time given by:

$$a(t) = \frac{v_{j+1}^f - v_j^f}{t} \quad (6)$$

The equation of motion is given by:

$$(v_{j+1}^f)^2 = (v_j^f)^2 - 2a(t)d_j \quad (7)$$

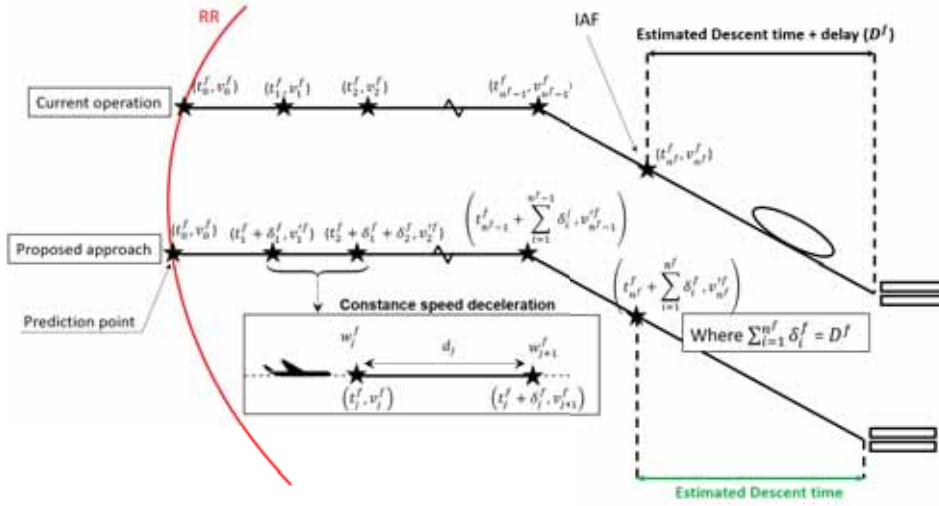


Figure 6. Concept diagram of the speed strategy approach.

where  $d_j$  refers to the distance between  $w_j^f$  and  $w_{j+1}^f$ . As  $v_{j+1}^f \neq v_j^f$ , the time  $t$  needed to fly from  $w_j^f$  to  $w_{j+1}^f$  is given by substituting equation 6 in equation 7 as follows:

$$t = \frac{2d_j}{v_{j+1}^f + v_j^f} \quad (8)$$

Finally, equation 8 is used to update the flight trajectory timing in each waypoint.

As we only manage flights inside the RR, the speed at the entry waypoint of the RR is a fixed parameter, and the speed control does not change it as shown in Figure 6.

Furthermore, our hypothesis is that flights should maintain the same landing performance as the actual operation. Therefore, they have to reach their instructed IAF with the same instructed speed. If not, they will need more time to land, and thus, it may yield to a disruption in the landing sequence, which in turn leads to the regeneration of delays. Therefore, the instructed speed at IAF is considered a fixed parameter.

2) *Conflict detection*: The airspace system includes both  $\mathcal{CF}$  and  $\mathcal{NCF}$  flights. While only  $\mathcal{CF}$  flights apply speed control maneuvers,  $\mathcal{NCF}$  are taken into account to evaluate the system performance and assure that the new flight trajectories remain conflict-free. In this work, we require a lateral separation of  $L_{sep} = 5$  NM and a vertical separation of  $V_{sep} = 1000$  ft. The network structure presented in Section VI-A complies with these separation norms as waypoints are separated by more than  $L_{sep}$  laterally and by  $V_{sep}$  vertically. Thus, conflict detection is restricted to nodes level.

Node conflicts are detected when aircraft flying over the same waypoint violate the standard separation norm. Let us consider two flights  $f$  and  $g$  flying over a waypoint  $WP_j$  such as  $f$  is ahead of  $g$ . The separation is ensured if the following equation is satisfied:

$$\Delta t = t_j^g - t_j^f \geq \frac{L_{sep}}{v_j^f} \quad (9)$$

Where  $v_j^f$  is the ground speed of the leading aircraft at  $WP_j$ , and  $t_j^f$  and  $t_j^g$  are the times where the flight  $f$  and  $g$  reach  $WP_j$ , respectively.

### 3) *Optimisation problem formulation*:

a) *Input data*: The optimization problem includes only  $\mathcal{CF}$  flights. Therefore, for each flight  $f$  belonging to  $\mathcal{CF}$ , the input data for the optimization problem are as follows:

- Actual trajectory points associated with the flight path:  $(w_j^f)_{j \in [1..n^f]}$ , where  $w_j^f$  is the 3D point trajectory points and  $n^f$  is the number of points.
- The flight speed profile  $(v_j^f, t_j^f)_{j \in [1..n^f]}$ , where  $(v_j^f)$  is the ground speed of  $f$  at the trajectory point  $w_j^f$ , and  $t_j^f$  is the time  $f$  flies over  $w_j^f$ .
- The predicted approach delay  $D^f$ .

b) *Decision variables*: Decision variables are defined by  $(v_i'^f)_{i \in [1..n^f]}$  where  $v_i'^f$  is the new assigned ground speed of each flight  $f \in \mathcal{CF}$  at the trajectory point  $w_i^f$ . It is illustrated by a set of speed rate of change ( $r^f$ ) for each flight  $f$ . Each  $r^f$  represents the percentage of change of  $f$  ground speed at its trajectory waypoint. It is defined as follows:

$$v_i'^f = v_i^f - (r^f * v_i^f) \quad (10)$$

As the flight achieved delay  $\delta_i^f$  is deduced from the flight speed rate of change  $r^f$ , we define the function  $g$  that evaluates achieved delay subject to the speed control measures as  $g(r^f) = \delta_i^f$ .

c) *Constraints*: In order to avoid excessive speed variation, boundaries are imposed on the variables ( $r^f$ ). The maximum and minimum allowed speed rate of change for the flight  $f$  are referred to as  $max_r^f$  and  $min_r^f$ , respectively.

In the present work, we propose to investigate two speed adjustment maneuvers. The first maneuver consists of reducing the aircraft speed by less than 10%. The second maneuver consists of changing the aircraft Mach by  $M0.02$  to  $M0.04$ . This adjustment range has been proposed in several previous works. As the aircraft Mach is not provided in the considered

data, we convert it into knots. This results in a speed adjustment range between 13 to 26 knots. Experiments show that this adjustment interval is also equivalent to a speed reduction rate ranging from 3% to 6%.

d) *Objective function*: In the current work, three main objectives are considered to be minimized. Let us first consider the following data:

- $\mathcal{N}$  the set of flights that apply the speed control strategy. Note that  $\mathcal{N} \subseteq \mathcal{CF}$ .
- $\delta_i^f$  the achieved delay by flight  $f$  between waypoints  $w_{i-1}^f$  and  $w_i^f$ ,
- $r^f$  the speed rate of change of the flight  $f$ , and
- $\mathcal{W}$  set of network waypoints.

The first objective function is illustrated in equation 11. It highlights the sum of the deviation between the achieved delay ( $\sum_{i=0}^{n^f} \delta_i^f = \sum_{i=0}^{n^f} g(r^f)$ ) and assigned delay ( $D^f$ ) over all flights.

$$obj_1 = \sum_{f \in \mathcal{N}} \left| D^f - \sum_{i=0}^{n^f} g(r^f) \right| \quad (11)$$

Note that we consider to minimize the absolute value of the difference between the predicted and absorbed delay so that the amount of absorbed delay will not exceed the predicted value. Furthermore, we aim at minimizing the flight approach delays with the least impact on aircraft performance. Thus, we consider minimizing the flight speed rate of change among all flights. Meanwhile, all flights with delays are required to participate in performing the speed control; thus,  $\frac{1}{N_f}$  is included, where  $N_f$  is the number of flights in the set  $\mathcal{N}$ .

$$obj_2 = \frac{1}{N_f} \sum_{f \in \mathcal{N}} r^f \quad (12)$$

Finally, the generated conflicts at each waypoint  $n$ , defined by  $\Phi_n$ , is also a criterion to be considered among the minimization objectives. Note that having a conflict-free solution is not a primer objective in our model. In fact, since we are tackling the cruise phase, the remaining conflicts can be handled by en-route controllers at the tactical level. Therefore, the number of generated conflicts is not a constraint in our problem; rather, it is included in the objective function to be minimized.

$$obj_3 = \sum_{n \in \mathcal{W}} \Phi_n \quad (13)$$

e) *problem statement*: The overall problem can be modeled as follows:

$$\begin{aligned} \min \quad & \alpha \sum_{f \in \mathcal{N}} \left| D^f - \sum_{i=0}^{n^f} g(r^f) \right| + \beta \frac{1}{N_f} \sum_{f \in \mathcal{N}} r^f + \gamma \sum_{n \in \mathcal{N}} \Phi_n \\ \text{s.t.} \quad & \min_r^f < r^f < \max_r^f \end{aligned} \quad (14)$$

where  $\alpha$ ,  $\beta$ , and  $\gamma$  are the parameters used to weight the minimisation of the three objectives  $obj_1$ ,  $obj_2$ , and  $obj_3$ .

### C. Simulated Annealing

Due to the high complexity of the present combinatorial optimization problem, we use a meta-heuristic algorithm—simulated annealing which has proved its potential in several ATM applications [14].

SA is widely known for its capabilities in avoiding getting stuck in a local minimum by implementing random neighborhood moves. SA is adapted to our problem as follows:

- 1) The *search space* consists of all flights belonging to  $\mathcal{CF}$  which involve a predicted delay higher than 2 minutes.
- 2) The *energy function* is given by the objective function of our optimization problem described in equation 14.
- 3) A *neighbor solution*  $\vec{x}_j$  represents a local change compared to a current solution  $\vec{x}_i$ . The process of getting a neighbor solution is divided into two steps. First, we select the flight to be modified based on the following heuristic: a random value  $p \in [0, 1]$  is generated according to a uniform law, then if  $p < 0.5$ , then the flight that involves the highest delay is considered, else, a random flight is considered. Once the flight to be modified is selected, a random value of speed change is assigned.
- 4) The *acceptance probability* of a neighbor solution  $\vec{x}_j$  is given by  $e^{(f(\vec{x}_i) - f(\vec{x}_j))/T}$ , where  $T$  is the temp,  $f(\vec{x}_i)$  is the objective value of the current solution,  $\vec{x}_i$ , and  $f(\vec{x}_j)$  is the objective value of the neighbor solution,  $\vec{x}_j$ .
- 5) A classical method for SA to decrease the temperature  $T$  is by applying a geometrical law given by  $T_i = a \times T_{i-1}$ .
- 6) The termination criterion is set when the temperature  $T$  goes below a predefined final temperature,  $T_f$ .  $T_f = b \times T_{Init}$  (with  $b \ll 1$  and  $T_{Init}$  is the initial temperature).

## VII. RESULTS & DISCUSSIONS

### A. Holding Detection and Prediction Models results

Using the proposed holding detection algorithm, all 679 flight trajectories withholding are correctly identified. Figure 7 plots the trajectories of 100 flights in which holdings were detected by the algorithm.

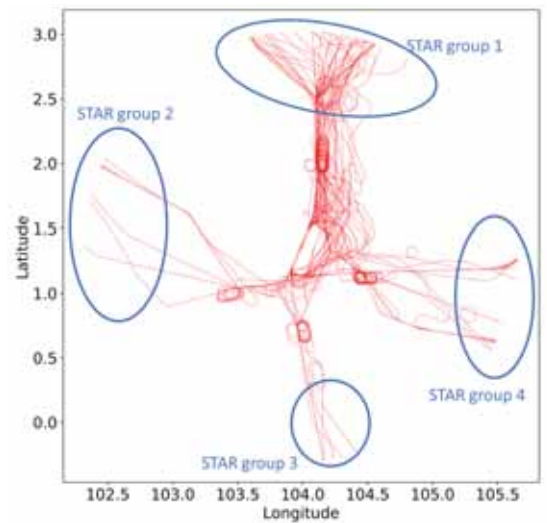


Figure 7. 100 trajectories with holding with the STAR groups

For all the prediction models, the data is split into 80% training data and 20% test data. In addition, during the training, three-fold cross-validations are performed to determine the optimal parameters for each prediction model. During the training of regression models (both for holding time and approach delay prediction), the trajectories are categorized into four Standard Terminal Arrival Route (STAR) groups, and each group has its own prediction model. The four STAR groups are shown in Figure 7. Flights that are approaching from the North, West, South, and East are categorized in STAR group 1, 2, 3, and 4, respectively.

The classification models are evaluated using the classification accuracy and the regression models with Mean Absolute Error (MAE) and Root Mean Square Error (RMSE).

1) *Holding Prediction*: The holding prediction model consists of a classification and a regression model. The classification model predicts whether an aircraft will be instructed to undergo holding during the approach. The prediction accuracy of the classification model on the test set is 92.9%.

The regression model predicts the aircraft holding time in the approach phase. Table II tabulates both the holding time statistics and the holding time prediction performance with and without using the predicted holding probability from the classification model. When the holding time prediction models do not make use of the predicted holding probability from the classification model, the RMSEs are comparable to the holding time standard deviations of the flights in the different STAR groups. However, when the holding time prediction models include the predicted holding probability, the RMSEs decrease at least 38%, and all the RMSEs are less than a minute. In addition, the predicted holding probability feature ranks the highest in the feature ranking.

TABLE II. HOLDING TIME PREDICTION RESULTS

	Holding time statistics (minutes)			Without holding probability		With holding probability	
	Total Flights	Mean	STD	RMSE	MAE	RMSE	MAE
STAR_grp 1	4186	0.448	1.485	1.414	0.725	0.870	0.281
STAR_grp 2	1958	0.143	0.899	0.885	0.279	0.364	0.081
STAR_grp 3	980	0.315	1.283	1.242	0.541	0.522	0.153
STAR_grp 4	2252	0.412	1.460	1.517	0.746	0.864	0.300

2) *Delay Prediction*: Similar to the holding prediction model, the delay prediction model also has a classification model and a regression model. Both the classification model and regression model make use of the predicted holding time from the holding time prediction model. The classification model predicts whether the aircraft will experience a delay of more than two minutes in the approach phase and the classification accuracy is about 69.5%. Even though the classification accuracy is not very high, we are more interested in the prediction accuracy of the regression model as the classification model only provides an input (i.e., the predicted probability that a flight will have delay more than two minutes) to the final approach delay prediction model.

The prediction results of the regression model are tabulated in Table III along with the delay statistics. Lesser data is used to train the delay prediction model as only delays for flights

with corresponding flight plans can be extracted. The RMSEs for prediction models that did not include the predicted holding time and the predicted delay probability is greater than three minutes for the four different STAR groups. On the other hand, the RMSEs for the second set of prediction models (which include the predicted holding time and predicted delay probability) are lesser than three minutes, except for one (i.e., STAR\_grp 3). Also, the prediction performance improves across all the four STAR groups. Furthermore, the predicted delay probability and predicted holding time are the top two features in the feature ranking.

TABLE III. DELAY PREDICTION RESULTS

	Delay statistics (minutes)			Without holding time and delay probability		With holding time and delay probability	
	Total Flights	Mean	STD	RMSE	MAE	RMSE	MAE
STAR_grp 1	766	2.952	3.990	3.311	2.547	2.373	1.669
STAR_grp 2	373	0.236	4.746	3.222	2.535	2.601	2.005
STAR_grp 3	337	4.173	4.067	3.905	2.762	3.181	2.233
STAR_grp 4	615	2.809	3.975	3.393	2.444	2.442	1.675

### B. Speed Control Results

The considered scenario involves both  $\mathcal{CF}$  and  $\mathcal{NCF}$  flights. The flight set includes 762 flights, among which 80 flights are belonging to  $\mathcal{CF}$  with predicted delays of more than 2 minutes. Those 80 flights are subject to speed control strategy, but while considering non-conflicting with remaining flights.

The objective function parameters are empirically tuned. The highest priority is given to reducing the delays (equation 11), thus,  $\alpha > \beta \geq \gamma$ . However, less priority is given to reducing the change of speed and conflicts. In fact, the speed adjustment range is operationally reasonable, thus relaxing this parameter is acceptable. Furthermore, minimizing the number of conflicts is less-weighted because as long as a low number of conflicts are generated, they can be tactically resolved by en-route controllers. The SA parameters are adjusted as a trade-off between achieved objective values and CPU times using a classic configuration.

The initial total delay is 513 minutes, with an average of 6.41 minutes per delayed flight. Experiments are conducted for three different RRs, namely 200 NM, 300 NM, and 500 NM, and for the two speed strategies discussed in VI-B3c. The first speed strategy, labeled SS 1, refers to the speed decrease rate of less than 10%. The second speed strategy, labeled SS 2, refers to the speed decrease rate ranging from 3% to 6%.

Figure 8 shows the percentage of absorbed and remaining delays within different RRs and different speed strategies. It is evident that the earlier speed control is applied, the more absorbed delays are achieved. Furthermore, increasing the range of speed adjustment (as in SS 1) yields more absorbed delays. For instance, at RR 200 NM, more than 20% of the total delays are successfully transferred to the cruise phase by applying speed control strategy 1, whilst, when applying speed control strategy 2, around 18% of the total delays are transferred to the cruise phase. Results from RR 300NM are quite similar to those from RR 200 NM. In fact, at RR 300 NM, about 30% and 20% of the total delay is transferred by applying SS 1 and SS 2, respectively. More



Figure 8. Absorbed and remaining delays within different RRs and different speed strategies for the considered scenario.

TABLE IV. DELAY STATISTICS FOR THE CONSIDERED SCENARIO IN MINUTES.

	Mean initial delay	Mean absorbed delay		Mean remaining delay	
		SS1	SS2	SS1	SS2
RR 200		1.39	1.01	5.02	5.38
RR 300	6.41	2.05	1.11	4.36	5.29
RR 500		4.38	2.67	2.02	3.73

noticeable results are recorded from RR 500 NM where almost 70% and 40% of the total delay is transferred to the cruise phase by applying SS 1 and SS 2, respectively.

Table IV summarizes the mean delay results after applying the two speed strategies. Initially, flights are delayed by almost 6.41 minutes on average. After applying both speed strategies, the average remaining delay decreases significantly with 2.67 and 3.73 average delay per flight when applying SS 1 and SS 2, respectively, at RR 500 NM. In terms of absorbed delays, it is found that by applying speed control at RR 200 NM, flights are able to absorb around 1 to 1.4 minutes of delays. The performance is slightly improved when speed control is applied at RR 300 NM, where flights can absorb on average from 1.1 to 2 minutes. More interesting results are recorded for speed control strategy at RR 500 NM. In fact, the average absorbed delay per flight can reach almost 4.38 minutes.

These experiments also evaluated the performance of our proposed approach in the presence of  $\mathcal{NCF}$  flights. However, since the speed adjustment range is narrow, it was found that no conflicts have been generated. This result is consistent with the fact that reducing flight speeds up to 10% can be performed without informing the controllers as it does not, usually, generate new conflicts. Thus, evaluating the conflicts at each algorithm iteration shows that the solution is conflict-free regardless of the speed adjustment applied.

## VIII. CONCLUSION

In this work, a method to transfer flight delays from the approach phase to the cruise phase is proposed. It includes an innovative holding detection algorithm to detect flight holdings and holding times from historical data. Furthermore, it presents a data-driven model that combines classification and regression prediction methods in order to predict flight holdings, the flight time of holdings, and flight delays at 200 NM away from the airport. Finally, it introduces

a speed strategy approach to absorb the predicted delays in the cruise phase. In order to evaluate the performance of proposed method, computational experiments are conducted using one month air traffic data for flights arriving at Singapore Changi airport. Two important observations were made. First, predicting flight delays is strongly correlated with the prediction of holding pattern and duration. Second, applying the speed control at 500 NM contributes to transferring up to 70% of delays to the cruise phase. This may help reduce the workload of TMA controllers as well as reduce fuel consumption caused by holding at lower altitudes.

In future works, we plan to investigate the holding and delay prediction models at RR 300 NM and RR 500 NM. Furthermore, the speed adjustment in the proposed model is fixed at the range ring and does not change up to the IAF. However, due to uncertainties, the delay initially planned to be absorbed may change over time. Thus, a dynamic speed adjustment will be investigated to better manage delay prediction errors or uncertainties.

## ACKNOWLEDGMENT

This research is supported by the National Research Foundation, Singapore, and the Civil Aviation Authority of Singapore, under the Aviation Transformation Programme. Any opinions, findings and conclusions or recommendations expressed in this material are those of the author(s) and do not reflect the views of National Research Foundation, Singapore and the Civil Aviation Authority of Singapore.

## REFERENCES

- [1] SESAR Deployment Manager, *Guidance Material for SESAR Deployment Programme Implementation*. 2017.
- [2] SESAR, "Extended arrival management (aman) horizon," 2014. Accessed on 30 July 2020.
- [3] Y. Glina *et al.*, "A tree-based ensemble method for the prediction and uncertainty quantification of aircraft landing times," in *AMS-10th Conference on AI Applications to Environmental Science*, 2012.
- [4] Z. Wang *et al.*, "Short-term 4d trajectory prediction using machine learning methods," in *7th SID*, 2017.
- [5] C. S. Kern *et al.*, "Data-driven aircraft estimated time of arrival prediction," in *IEEE SysCon*, pp. 727–733, IEEE, 2015.
- [6] L. Delgado and X. Prats, "En route speed reduction concept for absorbing air traffic flow management delays," *Journal of Aircraft*, vol. 49, no. 1, pp. 214–224, 2012.
- [7] Y. Matsuno *et al.*, "Analysis of achievable airborne delay and compliance rate by speed control: A case study of international arrivals at tokyo international airport," *IEEE Access*, vol. 8, pp. 90686–90697, 2020.
- [8] J. C. Jones *et al.*, "Stochastic optimization models for transferring delay along flight trajectories to reduce fuel usage," *Transportation Science*, vol. 52, pp. 134–149, 2018.
- [9] I. Dhief *et al.*, "Predicting aircraft landing time in extended-tma using machine learning methods," in *9th ICRAAT*, 2020.
- [10] M. Schäfer *et al.*, "Bringing up opensky: A large-scale ads-b sensor network for research," in *13th International Symposium on Information Processing in Sensor Networks*, pp. 83–94, IEEE, 2014.
- [11] Iowa Environmental Mesonet, "Asos-awos-metar data download."
- [12] EUROCONTROL, "Technical note: Algorithm to describe weather conditions at european airports."
- [13] A. V. Dorogush *et al.*, "Catboost: gradient boosting with categorical features support," *arXiv preprint arXiv:1810.11363*, 2018.
- [14] S. Alam *et al.*, "A distributed air traffic flow management model for european functional airspace blocks," in *12th ATM Seminar*, 2017.